Atomistic theory and computer simulation of grain boundary structure and diffusion

2000 J. Phys.: Condens. Matter 12 R497

(http://iopscience.iop.org/0953-8984/12/42/201)

J. Phys.: Condens. Matter **12** (2000) R497–R516. Printed in the UK PII: S0953-8984(00)08650-1

REVIEW ARTICLE

Atomistic theory and computer simulation of grain boundary structure and diffusion

Diana Farkas

Department of Materials Science and Engineering, Virginia Polytechnic Institute, Blacksburg, VA 24061, USA

Received 21 July 2000

Abstract. We present a review of the current state of atomistic theory and computer simulation methods in the study of grain boundary structure and diffusion properties. We review the multiplicity of possible local minimum energy structures that arise for the structure of the same grain boundary, particularly in the case of a grain boundary in an ordered alloy. We also review recent structural studies performed for randomly generated grain boundaries. The basic features of the interaction of vacancies with the grain boundary are reviewed for the case of special boundaries. We describe the use of a combination of molecular statics/Monte Carlo techniques for the calculation of diffusion properties along grain boundaries based on many-body interatomic potentials. The method is exemplified in the results obtained for a special grain boundary in the intermetallic compound NiAl. Finally, we describe the studies that have been carried out using molecular dynamics for special grain boundaries in fcc metals, showing that both vacancy and interstitial mechanisms may be important. The advantages and disadvantages of these techniques for the study of grain boundary diffusion are discussed.

1. Introduction

A very large body of simulation work has been devoted in the last three decades to the structure of high-angle grain boundaries in metals and alloys. In particular, symmetrical tilt grain boundaries have been the subject of many structural studies (see for example the excellent review of Sutton and Baluffi [1]). The implications of these studies for the general behaviour of grain boundaries have been discussed in many of these investigations [2–5]. Most of these studies are for special boundaries, as for example, series of symmetrical tilt boundaries or pure twist boundaries. These results may have more general validity, since the more general boundaries may be actually composed in part of combinations of structural units typical of the special boundaries [6]. These grain boundary studies have been performed using several techniques [7], most of which model special boundaries, depicting the grain boundary as a perfectly planar interface between two crystals with different orientation and rigid-body translated with respect to each other. As mentioned above, the two widely studied grain boundary types are pure twist boundaries and pure tilt boundaries, for which the misorientation between the grains is obtained through rotation around an axis that is either perpendicular or parallel to the grain boundary plane, respectively. Symmetrical tilt boundaries have been the most widely studied, especially for relatively low values of the reciprocal density of coincident sites, Σ, as defined in the classic coincident site lattice (CSL) model [8].

A large amount of work has been specifically devoted to studying the occurrence of cusps in the grain boundary energy values for the special misorientations that correspond to relatively

low values of Σ [8]. The occurrence of such cusps has only been established for the lowest values of Σ, the reciprocal density of coincident sites, and it seems clear that other grain boundary parameters, beyond the misorientation angle, will strongly influence the energy.

Sutton *et al* [7] studied the correlation of grain boundary energy with many of the possible grain boundary parameters. In that work, no correlation was observed with Σ, that is, no correlation with misorientation alone, independently of the choice of grain boundary plane. A certain degree of correlation was indeed observed with the planar density of coincident sites. A high planar density of coincident sites occurs for low values of the reciprocal density of coincident sites if the orientation of the grain boundary plane is such as to take advantage of the special misorientation. In this respect, Wolf [9] argued that low values of Σ are a necessary but not sufficient condition for an interface to be considered 'special'.

Recently, studies are emerging of more general boundaries, generated at random [10]. These, the first studies of the kind, show that even in randomly generated grain boundaries, there is a significant degree of order and that structural units that can be assigned to some special boundary appear in the more general structures. The study of random grain boundaries is now possible, due to the availability of increased computing power and more studies of this type are necessary in order to fully understand the nature of general grain boundaries.

The case of alloys, and in particular ordered alloys, poses separate problems since variations in local compostion and order are possible. The atomic structure of grain boundaries in ordered intermetallic compounds, especially transition metal aluminides, has been the subject of great interest, motivated by the the inherent brittleness of grain boundaries in such compounds. For example, structural applications of compounds such as NiAl are hampered by severe grain boundary brittleness. As part of this effort, there have been detailed atomistic simulation studies of grain boundaries in NiAl. Chen *et al* [11], Petton and Farkas [12] and Mishin and Farkas [13] simulated grain boundaries in NiAl and their interaction with point defects using the embedded-atom method (EAM) potential developed by Voter and Chen [32] for Ni_3Al. Fonda and Luzzi [15] and Yan *et al* [16] have studied the atomic structure of grain boundaries in NiAl using a Finnis–Sinclair type potential fitted to both the equilibrium properties of NiAl and the asymmetric behaviour of constitutional point defects in off-stoichiometric compositions. The study of Fonda and Luzzi [15] for the $\Sigma = 5$ [001] (310) boundary included a comparison between the simulated structures and an experimental study using high-resolution transmission electron microscopy (HRTEM). Yan *et al* [16] performed a simulation study that included several misorientations of [001] symmetrical tilt grain boundaries with both stoichiometric and off-stoichiometric structures. Some of this structural work included the interaction of the grain boundaries with point defects, which is most important for understanding the diffusion behaviour. Historically, it was first thought that grain boundaries and surfaces would act as perfect sinks for vacancies and other point defects. The structural simulation studies clearly show that this is not the case, but the energy of formation of vacancies will be lower in certain grain boundary sites than in the bulk. We note that no experimental evidence is available to verify the extent of these effects. The simulation results for vacancy formation energies should be analysed also in terms of their correlation with the local atomic environment, including the chemical composition of the atomic planes adjacent to the boundary. The study of such correlations of vacancy formation energies and local atomic configuration is of extreme importance in the understanding of the general behaviour of point defect–grain boundary interaction, and therefore grain boundary diffusion behaviour and mechanisms. For ordered alloys, the different atomic sizes may also play an important role in the nature of vacancy–grain boundary interactions. These size effects are believed to be important factors in grain boundary energetics, together with the ordering energy [17–19].

Excellent reviews [1, 7] exist on the structure of special grain boundaries in metals and in the structural part of the present review (sections 2 and 3) we will concentrate on recent developments regarding the role of the possible multiplicity of structures that may appear in a real material, and on the recent studies of random boundaries that are beginning to appear.

The investigation of atomistic aspects of grain boundary diffusion is much less advanced than the structural studies. The basic mechanisms are still poorly understood, and in particular the relationship among grain boundary structure and diffusion requires further study. The first atomistic models were proposed by Benoist and Martin [20, 21]. In their simple model the grain boundary is considered as a region with jump probabilities higher than those of the perfect lattice. This model is basically not supported by the structural studies of vacancy formation energies in various sites of the grain boundary. The structural studies that are now very advanced should serve as a basis for grain boundary diffusion models. This was done in some of the early molecular dynamics studies and in combined molecular statics/Monte Carlo simulations [22]. However, much work remains to be done in this area. In sections 4–7 we describe some of the latest results in vacancy–grain boundary interaction, molecular dynamics and combined molecular statics/Monte Carlo techniques for grain boundary diffusion.

2. The multiplicity of grain boundary structures

Most of the earlier grain boundary structural studies were primarily concerned with finding the lowest possible energy structure for a given grain boundary. This structure is usually referred to as the global minimum energy for that particular grain boundary. However, there may be several other minimum energy structures that are structurally different from the global minimum but that may have energies that are not much higher than the global minimum. These 'local minima' structures may then play a role in the actual structure in a real material. An additional source of a multiplicity of possible structures arises in the case of ordered alloys, where there may be variations in the local composition of the grain boundary region. Structural multiplicity was found in many metals and compounds and is reviewed for example by Balluffi and Sutton [23]. A simple way to understand the source of this multiplicity is to model it as it arises when different rigid-body translations are applied to one of the grains and the atomic configuration is relaxed after each translation. A detailed study of the structural multiplicity of grain boundaries in FCC metals has been performed by Rittner and Seidman [24]. In this type of study it is important to ensure that the cell of non-identical displacements is sampled completely and that the structures obtained are carefully analysed to identify strained variants of the same structure. Mishin and Farkas [13] developed a regular procedure for the identification of all non-identical stable structures of a grain boundary . The basic idea in that technique was to extend the so-called γ-surface technique to grain boundaries. This technique [25, 26] was originally introduced for the evaluation of the energetics of simpler translational planar faults in the lattice. In that context, the γ-surface technique is well developed, since it is important for dislocation emission processes. This technique, to find all the possible minima corresponding to a particular grain boundary, is now known as the grain boundary γ-surface, and is described in detail below. In the structures obtained by Mishin and Farkas using full relaxation from local minima of the grain boundary γ-surfaces, stable structures actually persisted in the broad vicinity of the minimum, while the residual shift was accommodated by elastic stresses in the lattice. The energy-versus-rigid translation behaviour observed seems to be governed by the balance between the grain boundary core energy and the elastic strain energy generated. Thus, most rigid-body translations around a stable configuration do not result in a new structure but merely induce a distortion of the existing structure and build up elastic stresses in the surrounding lattice. A transition to a different structure occurs when the local shear stress at

the boundary reaches a critical level, necessary to induce grain boundary sliding.

The various structures that can be created in this way, by rigid-body translations of one crystal with respect to the other, and the corresponding local minima of the energy functional, give rise to a series of possible grain boundary structures with nearby energies that may play an important role in a real crystal. Experimentally, this multiplicity has actually been observed for the case of $\Sigma = 5[100]$ twist boundaries in Au [27, 28]. Another case in which this multiplicity was observed experimentally is that of a $\Sigma = 3\ \langle 110\rangle\{112\}$ symmetrical tilt boundary in Cu_3Au [29].

An additional cause for the multiplicity of structures is present in ordered alloys when the crystallographic plane parallel to the boundary has different possible local compositions. In this case either of the two crystals can be terminated in any of the possible local compositions and this will typically give rise to different local compositions of the boundary structure. These different compositions will also significantly affect diffusion behaviour. In the case of these alloys the issue of how to calculate the grain boundary energy based on simulation results and how the grain boundary energy may depend on the overall bulk stoichiometry is somewhat complex, and we discuss it below.

As an example, we show in figure 1 three possible structures for the $\Sigma = 3\ \langle 110\rangle\{112\}$ symmetrical tilt boundary in Ni_3Al. These boundaries have different local stoichiometries. The boundary in figure 1(a) is created when a 100% Ni plane in one crystal is joined with a 50% Ni plane in the other crystal. This boundary maintains the overall stoichiometry of 75% Ni in the alloy, it can be referred to as a stoichiometric boundary or a 100/50 boundary. The boundary in figure 2(b) is created by joining planes for both crystals that are 100% Ni. This boundary contains, therefore, an excess of 1/2 Ni atom per boundary period and is Ni-rich. It can also be referred to as a 100/100 boundary. The boundary in figure 1(c) is created by joining two planes that are 50% Ni and is therefore Al-rich, with an excess of 1/2 Al atom per grain boundary period. It can also be referred to as a 50/50 boundary. The boundaries in figures 1(b) and 1(c) are off-stoichiometric.

2.1. The grain boundary γ-surface

For every grain boundary, the grain boundary γ-surface is defined calculating the grain boundary energy as a function of the translation vector which characterizes the rigid-body shift between the two crystals parallel to the grain boundary plane. These functions can in principle be calculated in two different ways: with full relaxation of the simulation cell and with relaxation only in the direction perpendicular to the boundary plane. This latter method corresponds to the grain boundary γ-surface.

Contour plots for a simple example grain boundary γ-surface are shown in figure 2 for a $\langle 001\rangle\{120\}\ \Sigma = 5$ grain boundary in NiAl [30]. For most grain boundaries in a series of symmetrical tilt boundaries with the [001] tilt axis [13], the local minima and maxima of the γ-surface were observed for translational states with either zero component along the tilt axis or with a relative translation of the grains by one half of the lattice parameter. In rare cases the γ-surface exhibited local maxima at intermediate translations. The γ-surface for each boundary was compared with the functional calculated with full relaxation. In that comparison, it was established that the difference between fully and partially relaxed grain boundary energies can be as large as a factor of two or more. Upon full relaxation, local minima of a γ-surface always transform to a local minima of the relaxed functional. If one local minimum of the γ-surface is deeper than the other, this relation is usually maintained after the relaxation. Translations corresponding to local minima always result in grain boundary structures which produce no long-range elastic stresses in the lattice. Every translation by

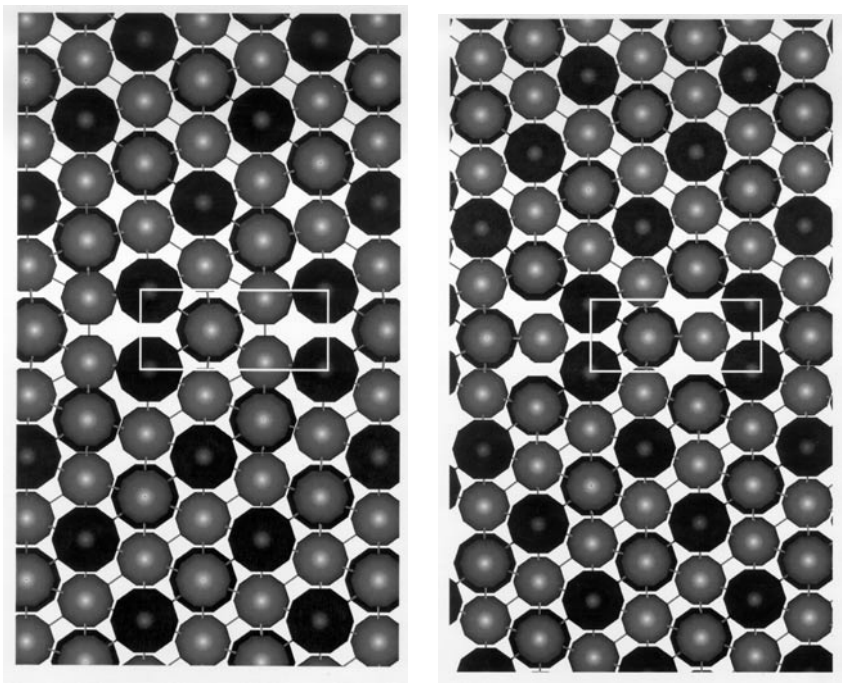

(a) (b)

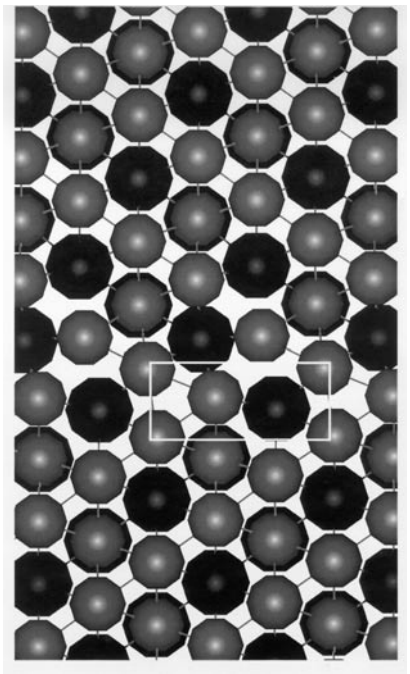

(c)

Figure 1. Three different structures of the $\Sigma = 3\langle 110\rangle 112$ symmetrical tilt boundary in Ni_3Al. The larger symbols represent Al atoms. (a) Stoichiometric or 100/50 structure. (b) Ni-rich or 100/100 structre, contianing an excess of 1/2 Ni atom per grain boundary period. (c) Al-rich or 50/50 structure, containing an excess of 1/2 Al atom per grain boundary period.

a vector near a local minimum results in essentially the same grain boundary structure with an additional shear distortion of the grain boundary core. Most of the residual translation is accommodated by elastic shear stresses in the region around the boundary. Local maxima of a γ-surface represent unstable states of the bicrystal. Subject to a translation by a vector that is near a local maximum, the grain boundary relaxes to a structure corresponding to the nearby local minimum.

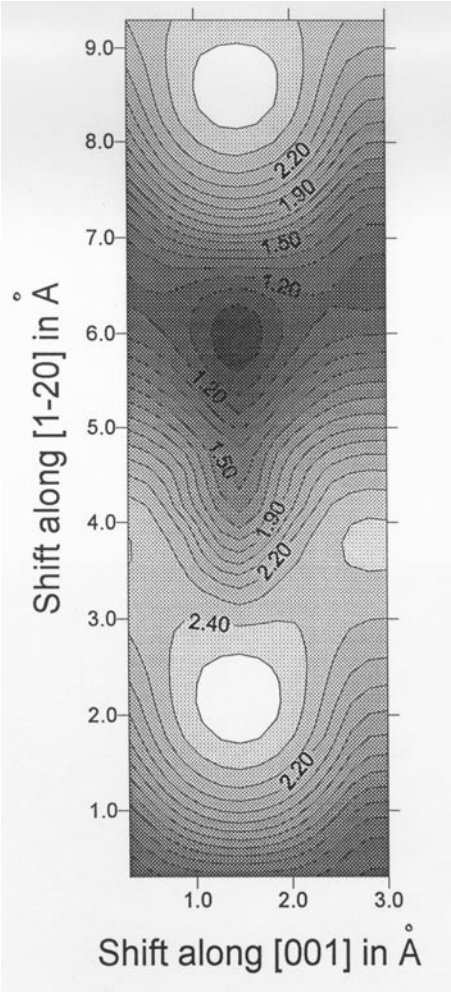

Figure 2. The grain boundary γ-surface for the $\Sigma = 5[001](210)$ symmetrical tilt boundary in NiAl, stoichiometric structure.

The grain boundary γ-surface technique is very useful in establishing the most stable, as well as metastable structures of a grain boundary. Such structures can be found by relaxing the simulation cell starting from the local minima of the γ-surface, followed by sorting out those grain boundary structures which are symmetrically related. The grain boundaries that were studied in the work of Mishin and Farkas [13] had, besides the ground state structure, typically 1–3 non-identical metastable structures. For the cases of ordered alloys, the grain boundary γ-surface should be calculated for each possible local stoichiometry available to the

particular boundary in question. This was done in the work of Mutasa and Farkas for a series of B2 ordered aluminides [30].

2.2. Calculation of grain boundary energies for off-stoichiometric boundaries in alloys

The simulation of any defect in an off-stoichiometric block alloy requires the calculation of the chemical potentials of the alloy components. In atomistic simulations based on the embedded atom method (EAM) scheme, one includes energy contributions due to mixed bonds, i.e. Ni–Al bonds in the case of NiAl and Ni_3Al. If the chemical potentials are calculated as cohesive energies of individual species in a perfect crystal, it is necessary to make some assumption on how the energetic contribution of mixed bonds will be assigned to each species. Once this assumption is made, the chemical potential is unique, as shown by Gao and Bacon [31]. In the early studies, the usual procedure was to use an equal splitting assumption for mixed bond energies. This assumption was used by Voter and Chen [14], in the development of the potentials for Ni_3Al, where it was necessary to calculate vacancy formation energies and in atomistic simulation of Ni_3Al grain boundaries [32, 33]. The equal splitting assumption was used in many other studies of the energetics of point defects, grain boundaries and surfaces. Recognizing that this assumption is arbitrary, Finnis and Hagen [34] proposed a scheme to obtain the chemical potentials using the thermodynamic definition. Essentially, their scheme recognizes that for an off-stoichiometric alloy, the reference state necessarily contains structural point defects. Therefore, the energy of the structural point defect that accommodates the deviation from stoichiometry should be zero. From this assumption, it is possible to calculate the chemical potentials for both components without the need for any assumptions regarding the splitting of the mixed bond contribution to the total energy. An additional complication arises in simulations using fixed boundary conditions where there is a separation of the energy of the free block from that of the fixed block. In this division, the computational procedure necessarily has to use some assumption for mixed bond splitting. This problem can be circumvented if the boundary of the fixed and free zones is of the same stoichiometry as the bulk. In this case, the resulting energies will not be dependent of the assumption made for splitting the mixed bond contribution to the overall energy of the block.

An important consequence of using the scheme proposed by Finnis and Hagen [34] is that the energies of various defects are now dependent on the stoichiometry of the total block in which the defect is embodied. For example, the energy of a free surface with a termination rich in Ni will be lower for a Ni-rich block than for a stoichiometric or Al-rich block. This is due to the fact that the chemical potentials are composition dependent quantities and have a discontinuity at the stoichiometric composition. Off-stoichiometric grain boundary energies will be dependent on the composition of the block in which they are; and the same is true for free surfaces. However, the cohesive energy of grain boundaries will not be affected by the stoichiometry of the total block since the cohesive energy is the energy change of converting a grain boundary into two free surfaces without any changes in block stoichiometry.

In table 1, we present the results of using this scheme for the calculation of point defect energies and surface energies in Ni_3Al using the Voter and Chen potentials [32]. Note that the value reported here for the energy of formation of Al vacancies corresponds to Ni-rich Ni_3Al and the value for Ni vacancies corresponds to Al-rich Ni_3Al.

Table 2 shows the results obtained for the energies of the $\Sigma = 3\langle 110\rangle\{112\}$ symmetrical tilt boundary in Ni_3Al.

The most important feature of these results is that there are several boundary structures that have very similar energies to the lowest possible energy obtained. For $\langle 110\rangle(112)$ symmetrical tilt boundaries, there are several different possible structures with calculated energies that differ

Table 1. Calculated chemical potentials and point defect energies in Ni_3Al using EAM potentials.

	Value using the equal bond splitting assumption (eV)	Value calculated using the procedure of [32] (eV)
μ_{Al} (Al-rich)	−4.83	−4.47
μ_{Al} (Ni-rich)	−4.83	−4.71
μ_{Ni} (Al-rich)	−4.51	−4.63
μ_{Ni} (Ni-rich)	−4.51	−4.55
ΔH_{vac} (Al)	1.8	1.96
ΔH_{vac} (Ni)	1.67	1.51
Anti-site Al in Ni site	0.46	0 (structural defect)
Anti-site Ni in Al site	−0.14	0 (structural defect)
{112} surface Al termination	1865 mJ m^{-2}	1805 mJ m^{-2} (Al-rich block) 1845 mJ m^{-2} (Ni-rich block) 1845 mJ m^{-2} (Stoichiometric block)
{112} surface Ni Termination	2014 mJ m^{-2}	2074 mJ m^{-2} (Al-rich block) 2034 mJ m^{-2} (Ni-rich block) 2074 mJ m^{-2} (Stoichiometric block)

Table 2. Energies obtained for several possible structures of the $\Sigma = 3\langle 110\rangle\{112\}$ symmetrical tilt boundaries in Ni_3Al.

Energy using the equal bond splitting assumption	Local boundary composition (number of excess atoms per period)	Energy in a stoichiometric block	Energy in an Al-rich block	Energy in a Ni-rich block	Cohesive energy
849	$\frac{1}{2}$ Ni	969	969	889	3129
851	1 Ni	1091	1091	971	3177
889	Stoichiometry	889	889	889	2990
903	$\frac{1}{2}$ Ni	1023	1023	943	3125
905	$\frac{1}{2}$ Al	865	785	865	2825
930	Stoichiometry	930	930	930	2949
1001	$\frac{1}{2}$ Al	961	881	961	2629
1026	Stoichiometry	1026	1026	1026	2853
1041	$\frac{1}{2}$ Al	1001	921	1001	2691
1150	Stoichiometry	1150	1150	1150	2729

by no more than 15% from the lowest energy structure. It seems possible that in the actual crystal more than one of these boundary structures will appear. One should remember that the present calculations were made by molecular statics at zero temperature. The entropy effects at finite temperatures may favour the appearance of different combinations of these structures along the grain boundary plane. This type of multiplicity of structures has actually been observed experimentally in a Cu–Au alloy with the same crystal structure as Ni_3Al [29]. Those experimental results are compared with simulation predictions by Farkas and Cardozo [35]. Although no studies have been performed to investigate the influence of the multiplicity of possible grain boundary structures on diffusion behaviour, it is expected that the presence of different structures will significantly affect diffusion.

Several of the calculated structures may possibly appear in the actual Ni_3Al crystal. Factors like local deviations from stoichiometry and segregation of impurities may also influence the

energetic balance between various structures and therefore determine the one with the lowest energy in a real crystal. Clearly, which grain boundaries will be lowest energy depends on the deviations from stoichiometry in the simulation block, i.e. the bulk stoichiometry in the material. It is also possible that an actual stoichiometric crystal will present a mixture of Ni-rich and Al-rich boundaries.

It is seen from table 2 that the Al-rich boundaries are actually lower in energy than the Ni-rich ones. This is contrary to what is obtained using the equal bond splitting assumption, due to the use of correct chemical potentials.

3. Structure of random non-special boundaries

Very few studies are available of the detailed atomistic structure of actually random grain boundaries. Van Swygenhoven *et al* [10] used two different procedures to create random boundaries: unconstrained and constrained stochastic methods. In the first procedure, the simulation cell volume was filled with nanograins grown from seeds with random location and crystallographic orientation; the space was filled according to the Voronoi construction. In the second procedure, the grain misorientations are still random, but constrained to values of less than 17°. The two procedures produce high-angle and low-angle random grain boundary samples, respectively. They studied pure Ni polycrystalline blocks and used a potential for Ni obtained from the work of Cleri and Rosato [36]. The Voronoi procedure gives irregular Vigner–Seitz polyhedra, whose faces, the grain boundaries, result randomly oriented as well. Samples were annealed using molecular dynamics computer simulation for few picoseconds at 300 K. Samples with various grain sizes were constructed using the same set of random locations and orientations, so the same microstructure appears, differing only in the scale of the sample (that is the number of atoms and therefore the grain size). This comparison allowed the study of the same crystallographic grain boundary for different grain sizes, up to 12 nm, isolating the effect of grain size on grain boundary structure.

All the grain boundaries that were analysed in that work showed a significant degree of order and structural features that were independent of the grain size. This fact suggests that the results for grain boundary structure will carry over to the realistic grain sizes found in polycrystals. In the grain boundaries that had misfits within a certain deviation from the perfect twin that they analysed (within about 10 degrees), they found that the grain boundaries contain a repeating building structure consisting of portions of $\Sigma = 3\langle 110\rangle\{111\}$ twin boundary, and steps. In the Ni sample with 12 nm grain size these blocks were repeated several times within the grain boundary plane. The same structure was found in the smaller grain samples, but with less or no repetition. For all other types of misfit, some kind of structural coherence was always observed. Misfit accommodation occured in a regular pattern, even in grain boundaries with high index common axis. As an example, figure 3 shows the structure of one of the random boundaries found in their work. The boundary characteristics are as follows: A misorientation between the two crystals that is given by a 25° rotation around a common axis which is close to a $[1\bar{1}0]$ type crystallographic direction, and a grain boundary plane which is close to [110] for the top crystal and $[77\bar{1}2]$ for the lower crystal. This is a non-special asymmetric boundary. It still presents a periodicity and certain planar density of coincident sites in the boundary plane. The period for this boundary within the boundary plane is quite small in the direction of the tilt axis, about 0.5 nm and it is about 3.87 nm in the direction perpendicular to the tilt axis. Although these are the first structural studies of randomly generated boundaries, they seem to indicate that the work that has been done over several decades on the structure of special boundaries will be of value, since the random boundaries tend to indeed present order and include some of the structural units found in the lowest Σ special boundaries. For low-angle grain boundaries,

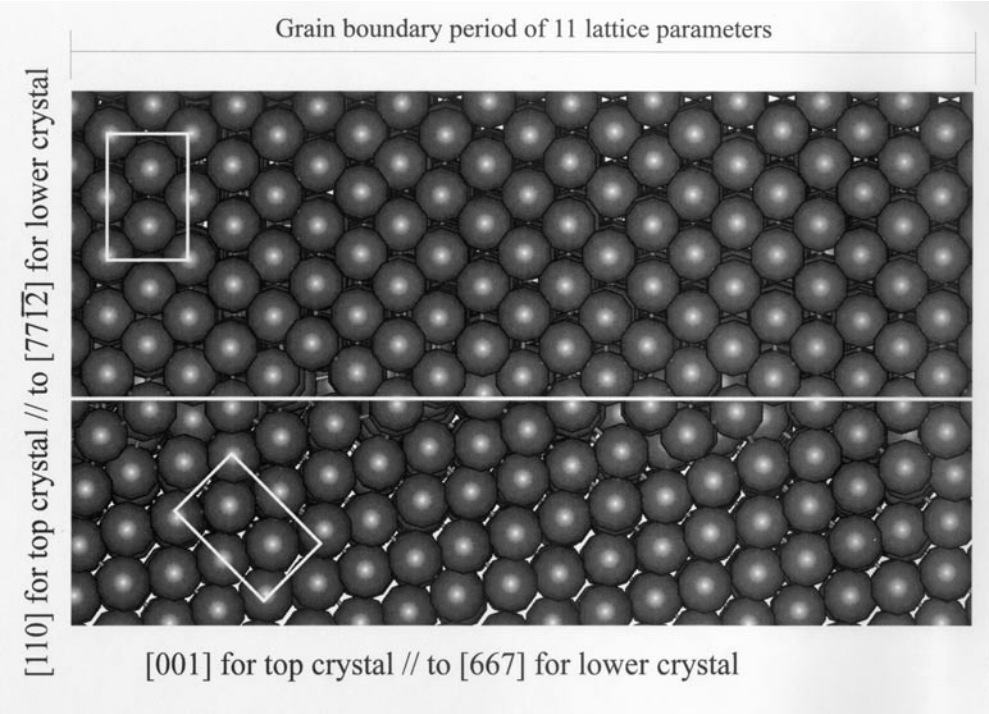

Figure 3. Structure of one randomly generated grain boundary, showing a high degree of order.

they observed typical regular dislocation patterns that are expected to accommodate the misorientation. The disordered regions that join the ordered domains may, however, play an important role in transport along the boundary. This issue requires further study.

4. Vacancy formation energies in grain boundaries

Lin and Chen [37] reported the interaction of various point defects with a grain boundary and found a general decrease in the point defect energy with respect to the bulk. They did not study the correlations of this decrease with the local grain boundary structure. In the work of Jang and Farkas [38], it was found that the anti-site formation energy in the vicinity of a grain boundary follows an oscillatory behaviour as a function of the distance to the grain boundary plane. Ordered alloys such as Ni_3Al ($L1_2$ structure) are expected to present such relaxations which can be understood as internal relaxations within the four atom motif that constitutes the Ni_3Al crystal when located at the nodes of a simple cubic lattice. That same work [38] also showed that segregation behaviour will vary with the composition and structure of the boundary in question. Al will segregate to the boundaries more easily than Ni as long as the boundary is not Ni-rich. The boundary tends to be a favoured location for disorder.

Ternes *et al* [39] calculated the vacancy formation energies for two possible structures of the $\Sigma = 3\langle 110\rangle\{112\}$ boundary in Ni_3Al. The structures they used corresponds to those of figures 1(b) and 1(c). A schematic picture of these grain boundary structures is shown in figures 4(a) and 4(b), including a label number given to each atom in order to identify its position within the grain boundary structure. These numbers are used in the following figures to show vacancy formation energies for the different atomic positions. Note that for both the 50/50

and the 100/100 boundaries, the mirror symmetry is broken due to the presence of structural vacancies. These structural vacancies are responsible for the configuration being Ni-rich or Al-rich. Also, because of the atomic environment, there are two non-equivalent types of Ni sites. In what follows, we reproduce the vacancy formation energy values calculated for the different sublattices, with sublattice 1 being occupied by Al (filled half-circles in figure 4). Sublattices 3 and 4 are both Ni and are equivalent to each other (squares in figure 4). Due to the presence of the boundary in the (112) plane, they are not equivalent to sublattice 2 (open half-circles in figure 4), which is also occupied by Ni. This can be readily understood if it is noted that the (112) planes are alternatively composed of sublattices 3 and 4 (100% Ni) and 1 and 2 (50% Ni). This equivalence is seen in both the relaxation displacements as well as vacancy formation energies, since it is dictated by symmetry.

Figure 5 shows the formation energy of vacancies as a function of location with respect to the grain boundary plane for the 100/100 boundary. The most favourable location for the vacancy is not in the atomic positions that delimit the structural unit, but rather on one of the two atoms that are contained in the centre of the structural unit. The other position in the centre of the structural unit, also on the grain boundary plane, is much less favourable. In the most favourable positions, the energy of formation of the vacancy decreased 31% from the bulk value. For the 50/50 boundary, the behaviour is shown in figure 6. In order to study correlations of the vacancy formation energy with lattice distortion, Ternes and Farkas studied the electronic density in the grain boundary region. The results showed no clear correlation among the local electronic density, as calculated by the EAM and the vacancy formation energy. Ternes and Farkas also plotted the trace of the dipole tensor, P, at each site defined as $P(i) = \sum_{j \neq i} F_{ij} \cdot R_{ij}$, where F_{ij} is the force vector exerted by atom j on atom i and R_{ij} is the vector joining atom j with atom i. This quantity indicates whether the particular site in the lattice is under tension or under compression. In a pure metal in equilibrium, it should always be zero for all atomic sites in the perfect lattice. In the Ni_3Al alloy, this quantity is positive for Ni atomic sites and negative for Al sites. The absolute values for Al are three times those for Ni, so that the total unit cell is in equilibrium. Al is a larger atom and it is under compression in the Ni_3Al unit cell whereas the smaller Ni atoms are under tension. It may be expected that the vacancy formation energy will correlate with the local tension or compression state in the grain boundary region. The results indeed showed some correlation with the vacancy formation energies. An important feature to be noticed in the results is the oscillatory nature of the vacancy formation energies plotted as a function of the distance to the grain boundary plane. This behaviour is consistent with the oscillatory behaviour found in the lattice relaxation displacements, as analysed by Savino and Farkas [40]. These oscillations are related to the effects of the pair interaction and volume dependent force at a surface. The competition among the forces result in these oscillations. This same competition can be seen as the explanation for the oscillations in the vacancy formation energies in the grain boundary region.

Most sites in the boundary present vacancy formation energies that are lower than the values for the bulk, meaning that the vacancy will be attracted to those sites. However, this is not true for all sites. The boundary contains certain sites for which the vacancy formation energy is actually higher than that for the bulk. The vacancies will be attracted to the boundary but only to certain sites in the boundary. Therefore, the boundary will not act like a true sink for vacancies, but rather only constitute a favoured region for the segregation of vacancies. Table 3 shows the maximum calculated segregation energies for vacancies in the two types of boundaries studied by Ternes and Farkas.

It is not clear in principle whether these results are generally valid for other, more special or more general boundaries. For example, the fact that the vacancy formation energies decrease

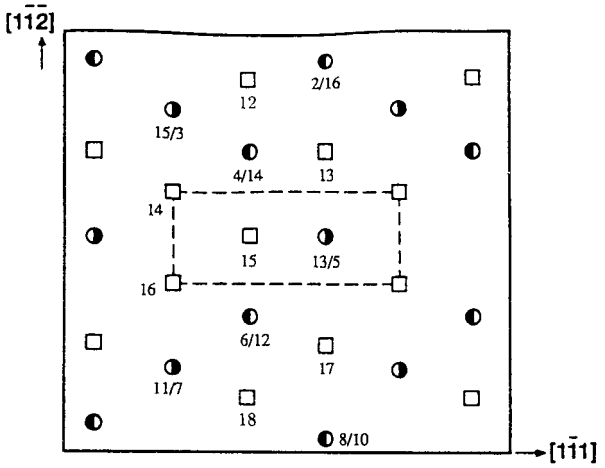

(a)

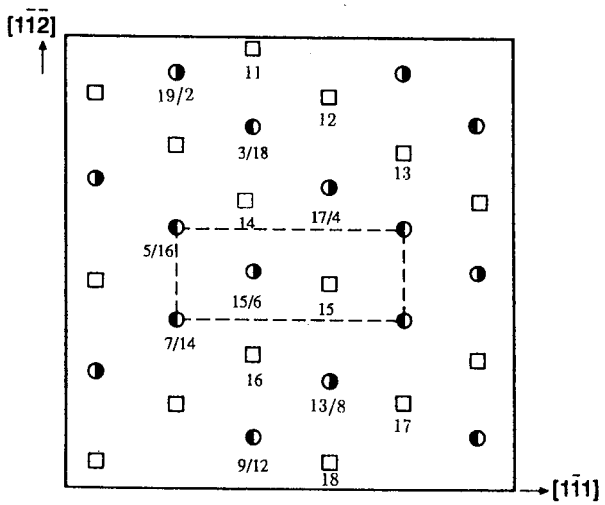

(b)

Figure 4. Schematics of two structures of the $\Sigma = 3\langle 110\rangle\{112\}$ symmetrical tilt boundary in Ni_3Al. These structures correspond to those labeled (b) and (c) in figure 1. The meaning of the symbols is as follows: filled half circles indicate Al atoms in sublattice 1, open half circles indicate Ni atoms in sublattice 2, and open squares indicate Ni atoms in sublattices 3 and 4. The atom numbers are for reference in the vacancy formation enenrgy calculations reported in figures 5 and 6.

Table 3. Maximum calculated segregation energies for vacancies in the two boundaries studied.

Vacancy type	Energy (eV)	
	100/100	50/50
Al	0.63	0.66
Ni I (sublattice 2)	0.40	0.25
Ni II (sublattices 3 and 4)	0.54	0.52

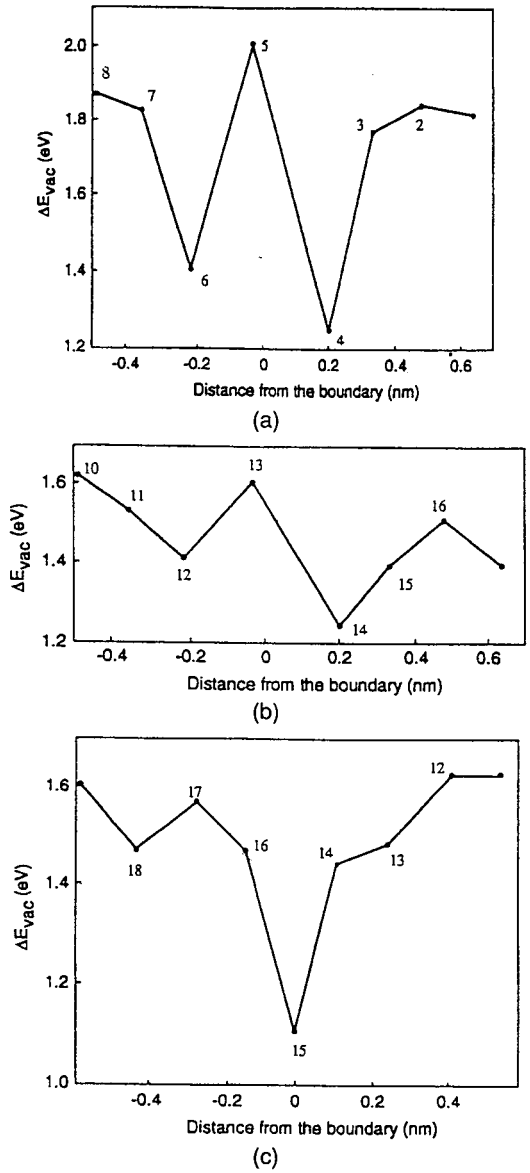

Figure 5. Vacancy formation energies in the grain boundary region for the two grain boundary structures of figure 4(a). (a) Al vacancies in sublattice 1. (b) Ni vacancies in sublattice 2(c) Ni vacancies in sublattices 3 and 4.

by about 20% in the boundary region may not be true for a more special boundary, like the $\Sigma = 3\langle 110\rangle\{111\}$ twin boundary where we expect segregation energies to be lower. It is expected that less special boundaries decrease the vacancy formation energy more than the more special ones, understanding a special boundary as one that has a high planar density of coincident sites [7]. It seems clear that the strength of the attraction between a vacancy and a grain boundary is strongly dependent on the details of the atomistic grain boundary structure, and will strongly vary from site to site.

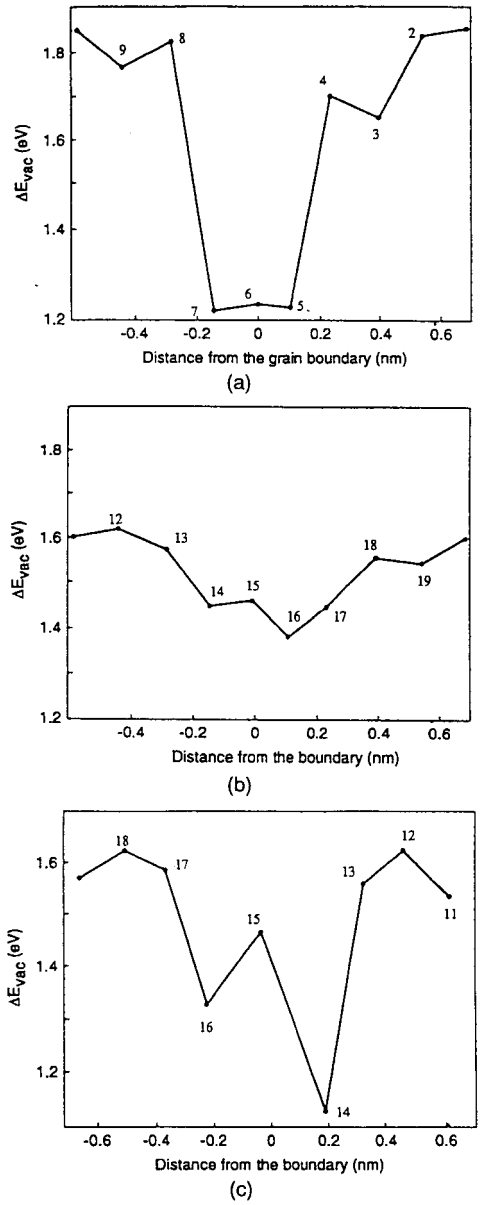

Figure 6. Vacancy formation energies in the grain boundary region for the two grain boundary structures of figure 4(b). (a) Al vacancies in sublattice 1. (b) Ni vacancies in sublattice 2(c) Ni vacancies in sublattices 3 and 4.

5. Monte Carlo simulation techniques for grain boundary diffusion

The Monte Carlo technique has been applied in the past to simulation of lattice diffusion, as for example in the work of Murch [41]. The method starts with an assumption of the basic probabilities and mechanisms of the diffusion process. Once a mechanism is assumed, as

for example a vacancy mechanism, the individual jump probabilities for the various types of possible jumps need to be known in advance. The method needs therefore to be coupled with another technique for calculating the jump probabilities. Usually, one can use molecular statics for the purpose of determining the activation energies of the individual jumps. In this process the technique relies on interatomic potentials, in the same way as the calculation of grain boundary structure may proceed. The atom that is performing the jump is not allowed to relax completely, but is constrained in various ways in order to efficiently obtain the energy of the activated state. Besides the activation energies calculated from statics simulations, assumptions need to be made about the attempt frequency for the various jumps. Once these assumptions are in place, the vacancy is then allowed to proceed in a random walk using the known jump probabilities. The diffusion coefficients can be evaluated from the random walk process, in a straightforward way.

Analysing this process, the drawback is precisely the assumptions about the mechanisms that have to be made *a-priori*. The advantage of the technique is that one can obtain excellent jump statistics, since the procedure is less computer intensive than the alternative, direct molecular dynamics. This is therefore an excellent alternative if one is confident about the diffusion mechanisms and one can accumulate much better statistics of the diffusion process. However, as we discuss below, establishing that confidence is not that simple for the case of grain boundary diffusion. These simulations are carried out using periodic boundary conditions, meaning that a jump out of the simulation blocks implies that the atom reappears at the opposite side of the block. Blocks of several hundred thousand atoms can be used.

Mishin *et al* [22] discuss two variations of the combined Monte Carlo/statics technique that can be used in this type of simulation for grain boundary diffusion. In the first variation of the technique the diffusion coefficient is calculated directly using the trajectories of the random walk effectuated by the vacancy or other point defect. In the second technique the diffusion coefficient is calculated in terms of the known local jump frequencies and the relevant correlation factors. It is these correlation factors that are in turn calculated using the Monte Carlo simulation method. The latter technique is more complex from a programming point of view but more efficient in the use of computer time. In the following section we discuss the results reported by Mishin [22] for diffusion in a special grain boundary in NiAl. In these results, it is important to keep in mind the main drawback of the technique, that is that the mechanism needs to be assumed *a-priori* and that the jump attempt frequencies need to be calculated using some simple approximation.

6. Diffusion in a $\Sigma = 5(210)[001]$ grain boundary in NiAl

Similar to the example of $\Sigma = 3\langle 110\rangle\{112\}$ boundary in Ni_3Al ($L1_2$ structure) discussed above, the $\Sigma = 5[001](210)$ boundary in the ordered compound NiAl (B2 structure) presents several possible stable configurations with different local stoichiometries. Diffusion calculations were performed by Mishin [22] for three different structures, one stoichimetric, one Al-rich and one Ni-rich. The formation energies of vacancies at different sites in the grain boundary were determined in a very similar way, as discussed in section 3. The values obtained for the energy of formation of vacancies in these boundaries were typically 0.25 eV lower than in the bulk for the most favourable sites and up to 0.15 eV higher than in the bulk for the unfavourable sites. Migration energies varied widely, depending on the type of jump considered, with values ranging from a very low 0.113 eV to values greater that 1 eV. The jump attempt frequency used for these calculations was assumed to be the same as that in the bulk. This value was obtained from the experimental measurements of Ni diffusion in the bulk. A probably more important limitation is that in the model, only vacancy jumps

within the same sublattice were considered. That is, no jumps were included that introduced disorder in the boundary and no consideration was given to the possibility of an interstitial type mechanism contributing to the diffusion process. Although these assumptions are crude and still have to be verified by other techniques, the results show important features that are expected to have some general validity. Figure 7 shows the results obtained in simulations of up to 300 000 atoms. The first important feature is that Arrhenius behaviour is indeed observed in a wide temperature range. We note that this is in contrast to the result obtained by molecular dynamics by Liu and Plimpton [42] for a grain boundary in Ag. The discrepancy can be explained by noting that the Monte Carlo simulations included only a vacancy mechanism whereas the low activation energy regime obtained by molecular dynamics was attributed to interstitial mechanism. Another important feature of the results shown in figure 6 is that there is a strong anisotropy in grain boundary diffusion, with diffusion along the tilt axis being faster than in the direction perpendicular to the tilt axis. Finally, for a fixed diffusion direction within the boundary, diffusion is fastest along a grain boundary enriched in the diffusing element. This conclusion may be related to the fact that only jumps within the same sublattice were included in the simulation. A result that will probably hold general validity that was obtained in this simulations is that there is no simple correlation of the activation energies obtained for diffusion in any of the directions and the activation energies of individual jumps. This means that in a general case, several different types of jumps can contribute to the overall diffusion coefficient. Furthermore, because of strong correlation effects, the jumps with the lowest activation energies may not be the ones that are dominant in the overall diffusion process. This point is illustrated in figure 8, where the correlation factor obtained is plotted as a function of temperature for Al diffusion in the NiAl grain boundary studied.

7. Molecular dynamics simulations

In the molecular dynamics (MD) technique one can directly determine the diffusion coefficient along the grain boundaries from the atomic trajectories generated as the defects migrate in the simulation. Since the MD technique follows the actual forces on the atoms as they migrate the obtained diffusion coefficient incorporates in a natural way correlation effects, entropy effects and other possible transformations in structure and/or mechanism that can occur with temperature. One very important advantage of this technique is that it does not require an *a-priori* assumption on the relevant diffusion mechanisms, the relative importance of various mechanisms can be studied as a result of the simulation.

As an example, Liu and Plimpton [42] studied the self diffusion of Ag in a special $\Sigma = 5(310)[001]$ grain boundary. They calculated the mean square displacement as a function of the MD simulation time and from the slope of these curves the diffusion coefficient was calculated at various temperatures. The results showed significantly non-Arrhenius behaviour, with the data falling in two different temperature regimes, with two different activation energies obtained from these results. The high-temperature activation energy obtained was 1.08 eV/atom, and the low-temperature one was 0.42 eV/atom. The transition was interpreted considering the fact that the two main factors contributing to the diffusion process, the defect formation energies and the defect migration energies. In the low-temperature regime it was speculated that interstitials dominate the process, since they have the lowest formation and migration energies. The vacancy-related mechanisms become important at higher temperatures. The activation energy data obtained in the study by Liu and Plimpton [42] for the high-temperature regime agreed well with the experimental values.

MD simulations of diffusion in a $\Sigma = 5(310)[001]$ Al tilt grain boundary were also performed by Liu and Plimpton [43]. They used three different potentials based on the EAM.

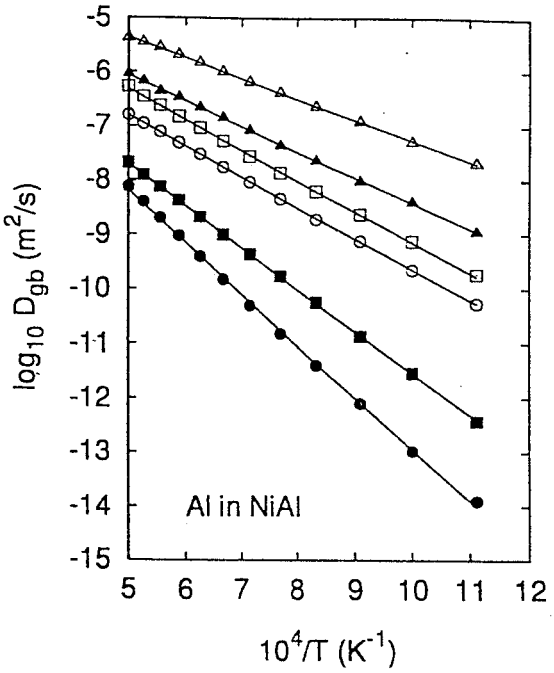

(a)

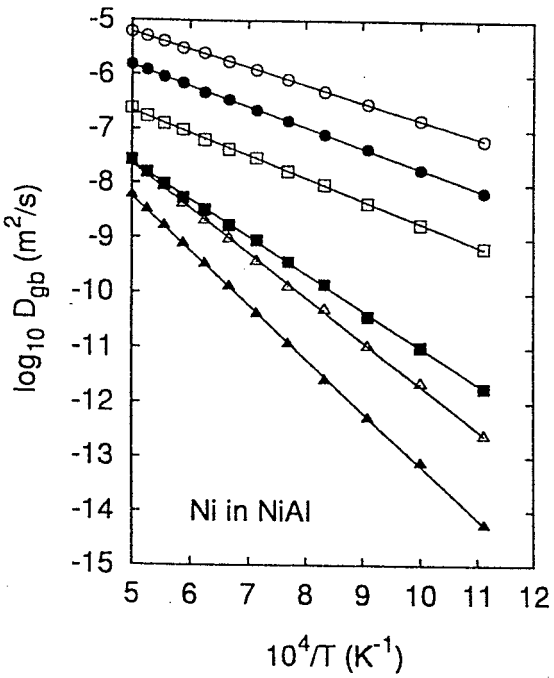

(b)

Figure 7. Difffusion calculations for the $\Sigma = 5[001](210)$ symmetrical tilt boundary in NiAl.

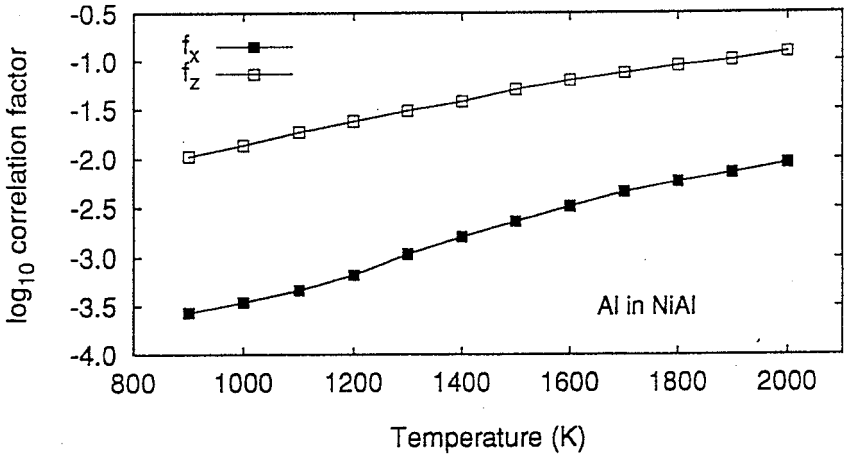

Figure 8. Correlation factors calculated for Al diffusion along the $\Sigma = 5[001](210)$ symmetrical tilt boundary in NiAl.

Their results were compared to experoimental data and they found that the EAM potentials that produce more accurate melting temperatures also yield activation energies in better agreement with experimental data. More recently, Liu *et al* [44] studied the defect generation and diffusion mechanisms in Al and Al–Cu alloys using molecular dynamics. These studies demonstrated that both interstitials and vacancies play an important role in grain-boundary mass transport via a Frenkel pair generation process. They showed that there are particular sites in this grain boundary where an interstitial and a vacancy can be created simultaneously in an energetically favourable way. The formation energy for such a Frenkel pair in the grain boundary they studied was surprisingly low, only 0.48 eV, which is comparable to the lowest vacancy formation energy (0.42 eV). This indicates that even under equilibrium conditions, grain-boundary Frenkel pairs should play a significant role.

Frenkel pair formation energies were also calculated for other grain boundaries, such as $\Sigma = 3\langle 110\rangle\{112\}$ and $\Sigma = 7\langle 110\rangle\{123\}$. The values are generally higher than those obtained for the $\Sigma = 5[001](310)$ boundary by 0.20 eV, but they are still comparable to the corresponding vacancy formation energies corresponding to these grain boundaries.

Once interstitials and vacancies are created via a Frenkel pair process, they diffuse along the grain boundary. The minimal energy barrier was calculated to be 0.28 eV for independent interstitial diffusion along the grain boundary and 0.26 eV for independent vacancies. The activation energies for individual jumps which are the sum of formation and migration energies and are calculated to be 0.76 eV for interstitials and 0.74 eV for vacancies. This is consistent with experimental results (0.74 eV) and molecular dynamics simulations (0.71 eV) for the same grain boundary.

Using an EAM format potential for Al–Cu they also addressed the effect of segregated Cu on the overall grain-boundary diffusivity in Al–Cu alloys. The migration barrier for a single Cu interstitial is calculated to be 0.81 eV. It is much higher than the migration energy for an Al interstitial (0.28 eV) in pure Al. On the other hand, the Al atoms surrounding the Cu interstitial experience much higher diffusion barriers than those in pure Al via a vacancy mechanism, with the lowest-energy barrier calculated being 1.10 eV. This indicates that Cu should be more mobile than Al in Al grain boundaries containing segregated Cu. Based on these results they were able to provide a possible explanation of why Cu prevents grain boundary

diffusion in Al–Cu alloys: Cu diffuses through bulk Al with an activation energy similar to that for Al self-diffusion and is driven by thermodynamic forces to segregate to grain boundaries. Cu prefers to segregate to the interstitial sites because of a smaller atomic radius compared to Al. Once Cu atoms occupy the interstitial sites, the overall grain boundary diffusivity is reduced as the stronger binding between Al–Cu plays a critical role to effectively increase the diffusion barriers for both Cu and Al migration.

These examples show that the molecular dynamics technique to study grain boundary diffusion can provide significant insight into the various mechanisms that operate in a particular grain boundary structre. The main limitation of the MD technique is the need for adequate statistics of atomic jumps. Since adequate statistics require long computational times, this technique is usually applied at high temperatures. However, with the ever increasing computing power available, more studies using this technique will certainly be done in the near future.

References

[1] Sutton A and Balluffi R 1995 *Interfaces in Crystalline Materials* (Clarendon Press: Oxford)
[2] Chen S, Srolovitz D and Voter A 1989 *J. Mater. Research* **4** 62
[3] Wolf D and Jaszczak J 1994 *J. Computer-Aided Materials Design* **1** 111
[4] Baskes M I, Foiles S M and Daw M S 1988 *J. de Physique Coll.* **49** 483
[5] Vitek V́, Wang G J, Alber E S and Bassani J L 1994 *J. Phys. Chem.* **55** 1147
[6] Sutton A and Vıtek V́ 1983 *Phil. Trans. R. London* A **309** 37
[7] Sutton A 1984 *Int. Metals Rev.* **29** 377
[8] Brokman A and Balluffi R 1981 *Acta Metall.* **29** 1703
[9] Wolf D 1985 *J. de Physique. Coll.* **46** 197
[10] Swygenhoven H V, Farkas D and Caro A 2000 *Phys. Rev.* B. **62** 831
[11] Chen S P, Voter A F, Boring A M, Albers R C and Hay P J 1989 *Mater. Res. Soc. Symp. Proc. Materials Research Society, Pittsburgh, Pennsylvania* **133** 149
[12] Petton G and Farkas D 1991 *Scr. Metall. Mater.* **25** 55
[13] Mishin Y and Farkas D 1998 *Phil. Mag.* A **78** 29
[14] Voter A F and Chen S P 1987 *Mater. Res. Soc. Symp. Proc. Materials Research Society, Pittsburgh, Pennsylvania* **82** 175
[15] Fonda R W, Yan M and Luzzi D E 1995 *Phil. Mag. Lett.* **71** 221
[16] Yan M, Vitek V́ and Chen S P 1996 *Acta. Materialia.* **44** 4351
[17] Farkas D and Rangarajan V 1987 *Acta. Metall.* **35** 353
[18] Kruisman J, Vıtek V́ and Hosson J D 1988 *Acta. Metall.* **36** 2729
[19] Takasugi T and Izumi O 1991 *Scripta Metall.* **25** 1243
[20] Benoist P and Martin G 1975 *Thin Solid Films* **25** 181
[21] Benoist P and Martin G 1975 *J. Physique* **143** 1357
[22] Mishin Y 1997 *Defect and Diffuison Forum* **C 4** 213
[23] Sutton A P and Balluffi R W 1995 *Interfaces in Crystalline Materials* (Oxford: University Press)
[24] Rittner J D and Seidman D N 1996 *Phys. Rev.* B **54** 6999
[25] Vitek V́ 1968 *Phil. Mag.* **73** 773
[26] Vitek V́ 1974 *Crys. Latt. Defects. Amorph. Mater.* **5** 1
[27] Oh Y and Vıtek VÍ986 *Acta. Metall.* **34** 1941
[28] Fitzsimmons M, Vaudin M and Sass S 1998 *Scripta Metall.* **22** 105
[29] Tichelaar F D and Schapink F 1988 *J. Physique.* **49** 293
[30] Mutasa B and Farkas D 1998 *Metall. Trans.* A **29** 2655
[31] Gao F and Bacon D J 1993 *Phil. Mag.* A **67** 275
[32] Farkas D, Savino E J, Chidambaram P, Voter A F, Srolovitz D J and Chen S P 1989 *Phil. Mag.* A **60** (4) 433
[33] Chen S, Voter A, Albers R, Boring A and Hay P 1990 *J. Mater. Research* **5** 955
[34] Hagen M and Finnis M W 1996 *Mater. Sci. Forum.* **207–209** 245
[35] Farkas D and Cardozo F 1998 *Intermetallics* **6** 257
[36] Cleri F and Rosato V 1993 *Phys. Rev.* B **48** 22
[37] Lin D and Chen D 1990 *J. Physique. Coll.* **51** 227

[38] Jang H and Farkas D 1990 *Grain Boundary Structure Simulation in Ordered Ni_3Al in J. Physique. Coll.* **51** 191–196
[39] Farkas D and Ternes K 1996 *Intermetallics* **4** 171
[40] Savino E and Farkas D 1998 *Phil. Mag.* A **58** 227
[41] Murch G E 1984 *Diffusion In Crystalline Solids* ed G E Murch and A S Nowick (New York: Academic Press) 379
[42] Liu C L and Plimpton S J 1995 *Phys. Rev.* B **51** 4523
[43] Liu C L and Plimpton S J 1995 *J. Mater. Research* **10** 1589
[44] Liu C and Borucki X Y L L J 1999 *App. Phys. Lett.* **74** 34